Techniques for Neutron Stress Determination with High Spatial Resolution

Thomas Gnäupel-Herold

Abstract A number of sub-surface strain measurement problems require spatial resolutions of the order of 10^{-1} mm to be meaningful. The use of neutron diffraction can be both time effective and otherwise advantageous compared to synchrotron diffraction if measurement directions and beam shapes are chosen such that scattered intensity is maximized. The first point refers to those directions and specimen orientations for which the gage volume orientation can be kept constant. They can be chosen such that preferred orientation boosts the diffracted intensity. The second point refers to the shaping of the incident beam for maximizing the illuminated volume in the material even for curved specimens. Guidelines and limitations of such high spatial resolution measurements are discussed.

Keywords Neutron diffraction · Sub-millimeter spatial resolution · Shaped aperture

1 Introduction

Many engineering problems require the non-destructive measurement of sub-surface strain fields that change significantly within millimeter length scales. For example, through-thickness residual stresses pose a big problem in sheet metal forming. With sheet thicknesses of ≈1 mm a depth resolution of ≈0.1 mm is required in order to reflect the strain gradient with sufficient detail. Because of primary beam flux and/or sufficiently low attenuation, neutron diffraction and synchrotron based high-energy X-ray diffraction (HEXRD) are essentially the only non-destructive methods capable of providing that resolution. Due to speediness of measurements and spatial resolution unmatched by neutron diffraction HEXRD represents the predominantly used experimental tool for the evaluation of strain gradients up to the scale of 1 mm [1–4]. The main problem associated with HEXRD is that Bragg angles of usable reflections become small—of the order of 10°—which leads to a high-aspect ratio intersection of incident beam and reflected beam (gage volume) with lengths up to 1 mm and a corresponding loss in spatial resolution in this direction. This problem is exacerbated for high-Z materials that require photon energies up to 100 keV and more to achieve sufficient depth penetration. Another problem is the size of the gage volume which is of the order of 10^{-2} mm^3 [2]. The actual volume of grains that fulfill the diffraction condition and scatter into the detector is much smaller (of the order of 10^{-6} mm^3), and this has implications both for continuum-based calculations of quantities such as elastic constants, and for the measured d-spacing. For example, due to insufficient elastic constant averaging stress fluctuations of ±5% from the average can be expected for ferritic steel if the number of contributing grains is <100 [5]. Regarding the d-spacing one has to expect deviations not related to stress from one measurement location to the next because the center of gravity of the contributing grains within the gage volume changes.

These considerations together with source availability—only 3rd generation synchrotron sources offer the necessary flux and photon energy range—make neutron diffraction an attractive technique for depth-resolved strain scanning. Here, the limitations are of a different nature. Primarily stemming from the low primary beam flux, gage volumes

T. Gnäupel-Herold
University of Maryland, College Park, MD 20742, USA

T. Gnäupel-Herold (✉)
NIST Center for Neuron Research, Gaithersburg,
MD 20899-6102, USA
e-mail: tg-h@nist.gov

are typically >1 mm³ which implies that the spatial resolution is available only in one or two dimensions [6], thus limiting the range of materials problems suitable for study with neutron diffraction. It should be mentioned that some efforts were made to increase the neutron flux at the sample position through the use of neutron lenses based on total reflection in bent, hollow fibers [7, 8]. However, due to several factors such as insufficient gains in the focal point, large beam divergence (affecting the peak width), and high manufacturing cost such a device has not yet been used for depth resolved strain measurements with neutrons.

As outlined in the following, for a problem suitable for study with neutron diffraction the experimental conditions can be chosen such that, using simple aperture systems, depth resolutions are ≈0.1 mm at data collection times of the order of minutes per orientation and location.

2 Experimental Technique

The practice of using flat gage volumes in sub-millimeter spatial resolution strain measurements is quite common at neutron sources. The incident and reflected beam apertures define a gage volume of the shape of a wide but thin parallelepiped, and it is used to scan the strains caused by a plane stress field that varies with depth. The extension of this technique to more complex specimen shapes and stress fields is outlined in Fig. 1.

The overriding goal of the method is to produce a high spatial resolution in one specimen direction while providing a gage volume of several mm³ for sufficient scattering intensity. The orientation of the gage volume with respect to the individual specimen orientations is constant. It is worth noting that the constant gage volume orientation has an equivalent in (surface) X-ray diffraction where the beam spot is kept constant in orientation and size [9]. The measurement procedure consists of a set of individual through-thickness strain scans where each scattering vector orientation (φ, ψ) is produced by means of a combination of specimen orientation, aperture orientation (rotation about the beam axis), and a different Bragg angle θ (produced by a different wavelength). The ability to reproduce a wavelength with sufficient accuracy is lacking on many neutron instruments; hence it is necessary to measure a reference sam-
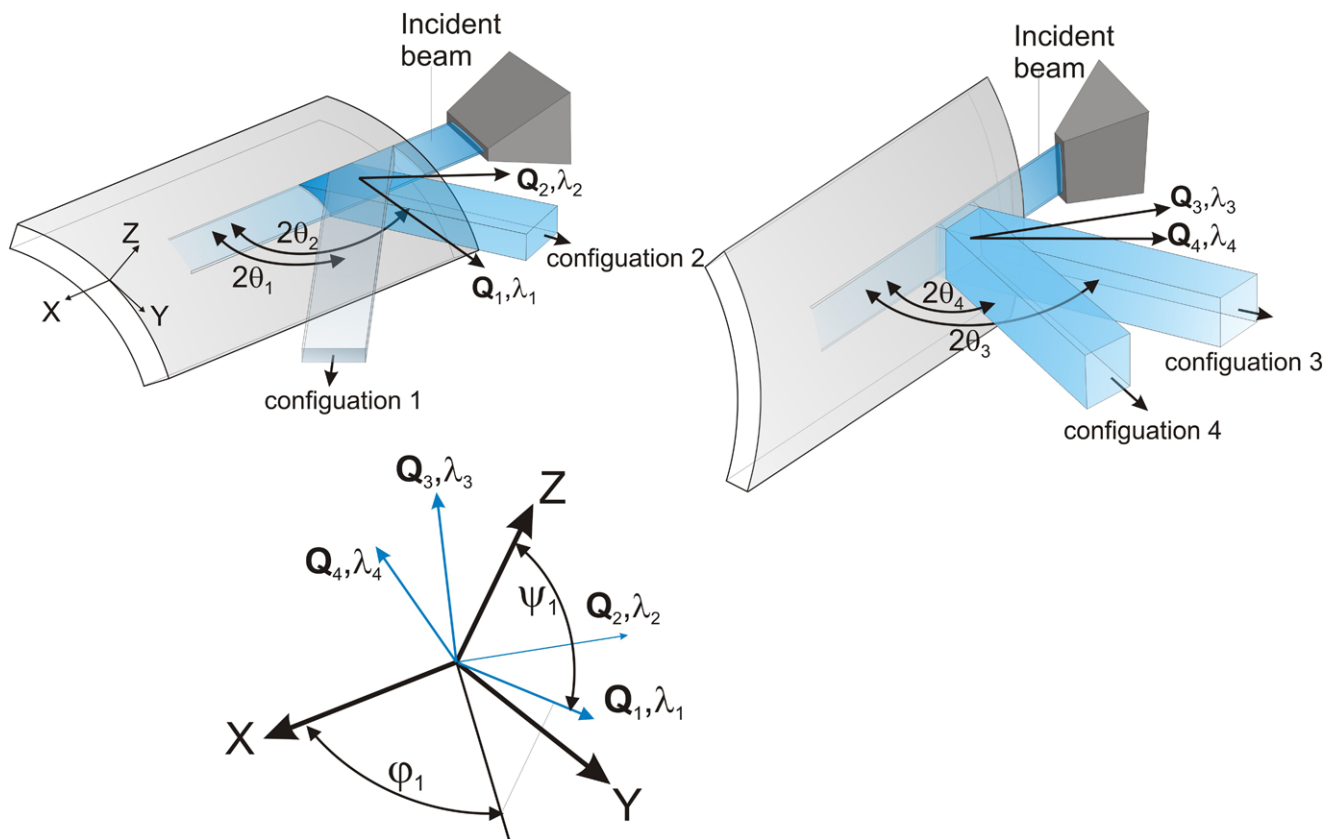

Fig. 1 The combination of rotations of the specimen, rotation of the aperture (primary) and different 2θ-values (through different wavelengths) result in different orientations of the scattering vector **Q**. The picture can be understood as the incident beam rotating together with the sample to produce different orientations while maintaining both the spatial resolution (in the depth direction Z) and the depth coordinate (Z) of the gage volume
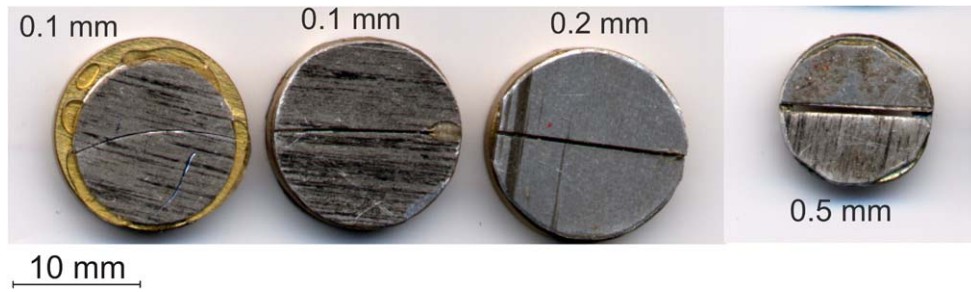
Fig. 2 Upstream (towards monochromator) and downstream (near sample) parts of primary aperture systems with cadmium used as a neutron absorber. The front end part produces a specific beam shape (see the curved aperture on the *left*) while the upstream part (towards the monochromator) limits the divergence. The combination of aperture openings, their distance to each other, and the specimen distance determine the effective spatial resolution
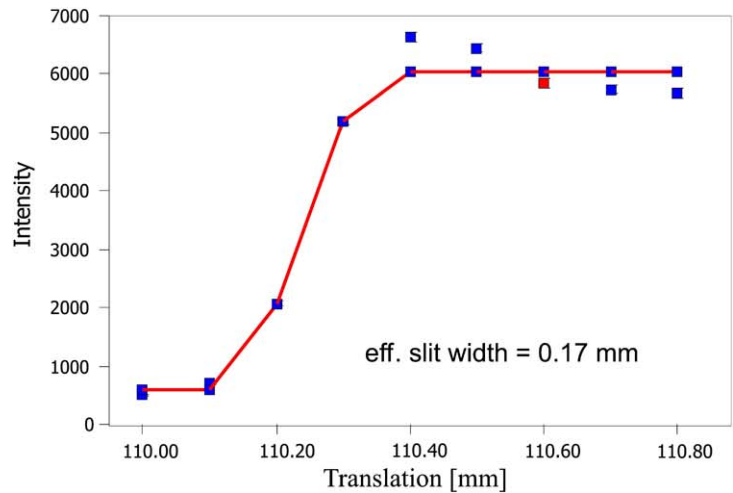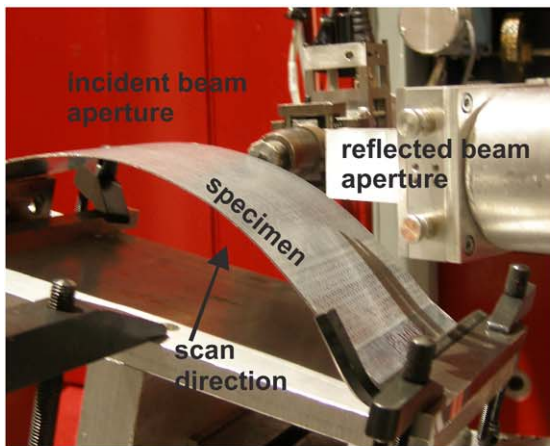

Fig. 3 Stepwise translation of a curved specimen into the gage volume (entering curve). The uncertainties are of the order of the size of the symbols

ple or unstressed d_0-sample at each aperture orientation and each wavelength. The requirements for measurement uncertainties are significantly higher for reference measurements; hence, this will add significantly to the total data acquisition time. The incident beam is subject to attenuation; thus, the location of the gage volume should be as close as possible to the face through which the beam enters the sample. The guiding principle should be to avoid the disturbances of the stress field near the edge. For example, for sheets with 1 mm thickness it is deemed sufficient for the outer edge of the gage volume to have a distance of $3\times$ sheet-thickness (3 mm) from the edge of the specimen. It is also to be expected that attenuation causes the center of scattering to be shifted from the center of the gage volume; this requires that the reference sample reproduces the attenuation conditions of the specimen (same material, same aperture distance and gage volume location).

Another feature shown in Fig. 1 is that the primary beam enters the specimen in a direction of symmetry for the specimen. This way it is possible to shape the primary beam such that it follows the outline of the specimen surface. In practice this is done by cutting thin cadmium-sheet along the specimen shape using razor blades. This procedure allows it to produce almost arbitrary beam shapes. A selection of apertures is shown in Fig. 2.

The alignment of the slit with respect to the specimen surface (curved or flat) is done visually. The main purpose of the shaped slits is the increase of the gage volume without the loss of spatial resolution that would otherwise occur for curved specimens. With good alignment of the beam tilt and beam axis to the specimen tilt and specimen axis it is possible to achieve a spatial resolution <0.20 mm as demonstrated by the entering curve in Fig. 3. A data acquisition time of 1000 s was necessary to achieve a strain accuracy of $<10^{-4}$ in the configuration shown in Fig. 3. The intensity of the beam diffracted from the gage volume as the specimen enters the gage volume defines a function that is fitted to the integrated intensities of the Bragg peak at each translation step [10]. The parameters of this function are the surface position, the Bragg angle (fixed), the attenuation (for a
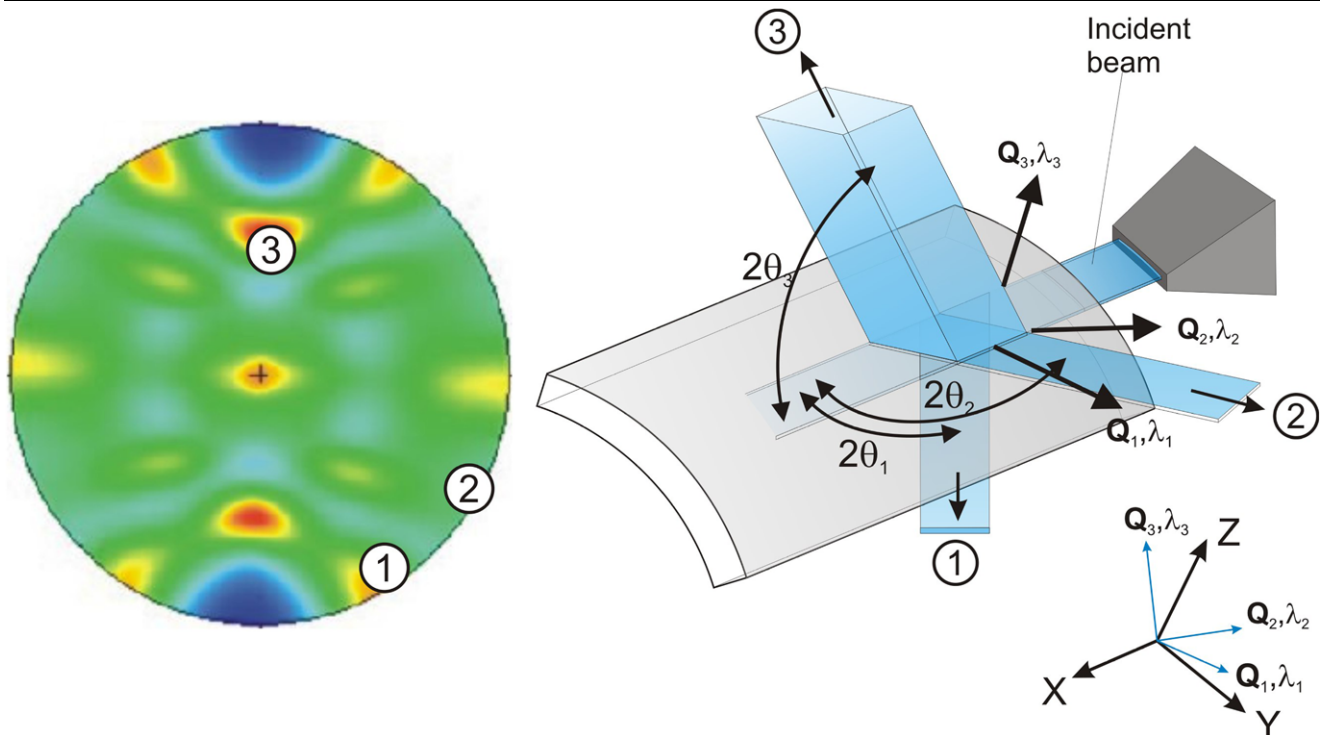
Fig. 4 Measurement configuration and orientation of the scattering vectors in the (211) pole figure of a AISI 1010 ferritic steel (*left*). The axial (*X*) distance of the gage volume from the sample surface should be as small as possible; here, the closest edge of the gage volume had 3 mm (3× thickness) distance to the face of the sample

geometry in which the scattering vector is not parallel to the sample surface) and the effective slit width. The effective slit width defines the effective size of the gage volume and it gives a measure of the spatial resolution.

In order to achieve the resolution shown in Fig. 3 it is necessary both to limit the beam divergence (here: 0.1°) by means of additional upstream slits and a minimal distance between the primary slit and the gage volume location in the specimen (here: 10 mm from edge). Thus, the primary slit is usually as close as possible to the specimen (here: 1 mm). There are no such strict requirements for the diffracted beam slit. The opening is typically chosen to be equal to the larger opening of the primary slit and the slit distance should be as close to the specimen as possible.

Further increases of the scattered intensity can be achieved by taking advantage of preferred crystallite orientation through measuring in directions of the intensity poles. This is outlined schematically in Fig. 4 for the (211) reflection on a ferritic steel sheet metal. The specimen had undergone rolling and stretch-bending resulting in a roughly cylindrical shape. The corresponding pole figure is shown on the left side.

Different orientations of the scattering vector **Q** are achieved by combinations of different specimen orientation and Bragg angles through different wavelengths. The incident beam is aligned such that it is parallel to the surface in the direction of the cylinder axis and, defined by the slits shown in Fig. 2, the beam has the same curvature as the specimen. For most neutron diffraction stress diffractometers the angle 2θ is varied (detector rotation) in the horizontal plane which is defined in Fig. 4 by the incident beam and the directions (1) and (2). The directions (1) and (2) of the diffracted beams can be measured in the same specimen orientation shown in Fig. 4. The direction (3) requires that both the specimen and the primary aperture are rotated together (see Fig. 1, right).

This approach requires the ability to change the wavelength of the neutron beam such that the neutron beam is diffracted at different Bragg angles θ with the goal of matching the direction of the scattering vector **Q** to the direction of increased intensity in the pole figure. Changing the **Q**-direction through the wavelength comes with one drawback: on some neutron diffractometers the instrument parameters do not allow the determination of the wavelength with sufficient accuracy, thus requiring a calibration for each change of the wavelength or the measurement of the specimen reference (unstressed) d-spacing. Both require comparable amounts of measurement time. Additional time is needed to establish the position of the surface for each orientation. The initial position accuracy from optical alignment is <0.5 mm; however, in order to achieve an accuracy better

than the spatial resolution it is typically necessary to perform a wall scan (entering curve) [10].

The range in the space of **Q**-orientations is reduced by the constraints posed by usable Bragg angles (typically 30° to 70°), by the directions of intensity poles, and by the requirements of the specimen symmetry and shape. For example, for optimal spatial resolution in the thickness direction a cylindrically curved specimen with a curved neutron beam as shown in Fig. 4 must be oriented with the cylinder axis parallel to the direction of the incident beam. If the specimen is a flat sheet then there is greater flexibility in selecting measurement directions; for example, both the principal in-plane directions X and Y are accessible. However, regardless of the specimen shape the perpendicular direction Z cannot be measured since this would require a very small Bragg angle outside of the range that can be produced by wavelength changes. It should be noted also that since the azimuth φ and tilt ψ (see Fig. 1 for definition) are generally non-zero the data analysis excludes simple $\sin^2\psi$ linear regression [13] for stress determination and it is required to fit all components of the stress tensor [14] or to make explicit assumptions about their magnitude. For example, thin sheets with ≈ 1 mm thickness usually justify setting the normal stress component to zero.

3 Examples

3.1 Side Panel of a U-Channel

The experimental technique outlined above was successfully used to determine the trough-thickness stress distribution in deep drawn U-channel sections shown in Fig. 5 with the geometry and sample shown in Fig. 3, left. The

process and background of the forming process is described in [11, 12].

The stress gradients are resolved in good detail which, together with the surface stresses determined by X-ray diffraction, indicates a spatial resolution that is sufficient to indicate the character of the gradients present in the sheets. Figure 5 demonstrates that neutron diffraction can be successfully used for the non-destructive investigation of subsurface strains for a class of materials that previously were the domain of destructive methods (X-ray diffraction with layer removal) or HEXRD. These materials include especially steels, both ferritic and stainless/austenitic and nickel based alloys. Compared to these materials aluminum alloys have a small coherent neutron scattering length resulting in reduced scattered neutron intensity while exhibiting a much reduced X-ray absorption, thus making depth gradients of strains in aluminum and its alloys more suitable for investigation with HEXRD [3].

3.2 Laser-Peened Steel Plate

Laser peening generates very high stresses in less steep gradients than peening through mechanical impact; thus it is well suited for a comparative study of the method. The specimen was a 300M steel, with dimensions 42 mm × 47 mm × 13 mm. For this sample, two different measurements were taken: one measurement (1) followed the procedure outlined here with the flat (6 mm × 6 mm × 0.2 mm, 8 mm from both edges) gage volume having a constant orientation with respect to the specimen surface. The second (2) measurement followed the established procedure of a neutron diffraction stress measurement in which a matchstick-like gage volume (0.5 mm × 0.5 mm × 20 mm) was used. All measurements
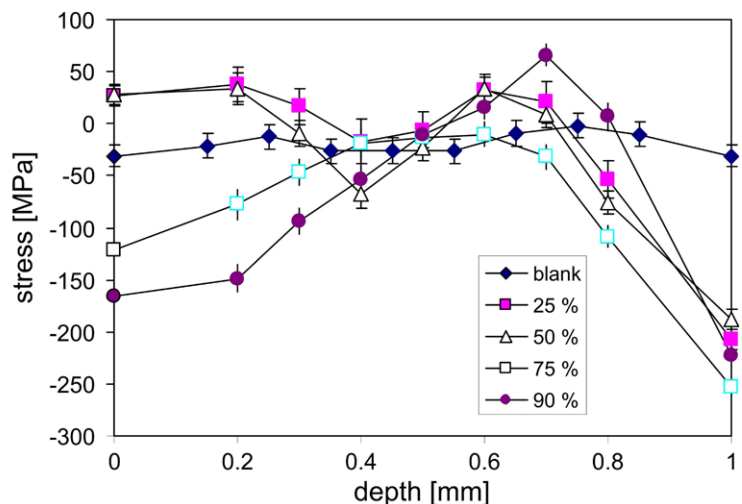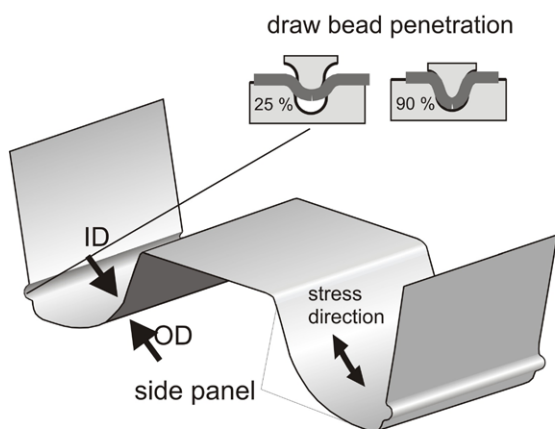

Fig. 5 Through-thickness stress (**b**) in the side panel of a deep drawn U-channel in the tangential direction (**a**). The values directly at the surface (0 mm, 1.0 mm) were determined by X-ray diffraction
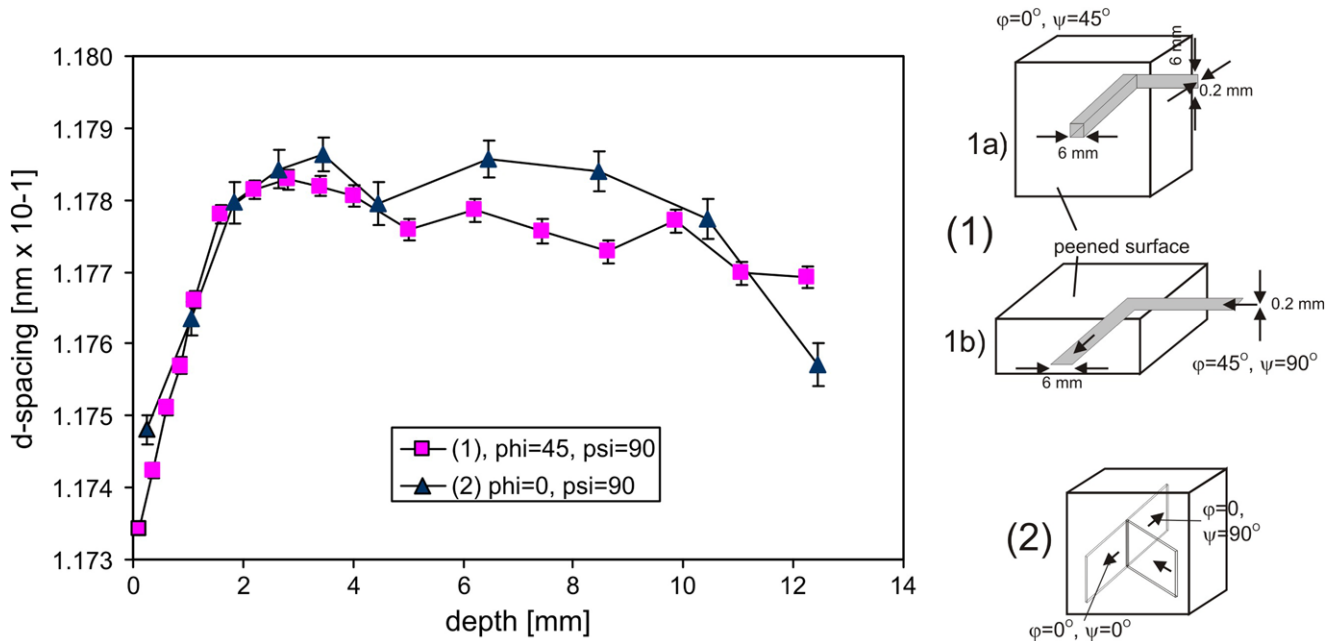
Fig. 6 D-spacings in two in-plane directions for method (1) and (2). Specimen and gage volume orientations are shown on the right

were referenced to the *d*-spacing measured on iron powder. No unstressed sample or coupon was available, therefore, a d_0 was used from a calculated value for the location closest to the surface where $\sigma_{zz} = 0$. Specimen orientations and *d*-spacings measured in comparable orientations are shown in Fig. 6. It was confirmed using surface X-ray diffraction that $\sigma_{xx} \cong \sigma_{yy}$ for the entire surface including the measurement locations used here. Also, at locations with distances ≤3 mm from an edge the surface stresses start to decrease. The location for (1) was safely outside that zone (8 mm distance).

The use of the geometry in 1b) (Fig. 6, right) is certainly not new but using the same primary beam, only rotated, as in geometry 1a) has not been reported to the best knowledge of the author. Geometries 1a) and 1b) together give a constant orientation of the gage volume within the sample, and with constant spatial resolution.

The near surface differences in *d*-spacings in Fig. 6 can be interpreted as the result of a smoothing effect of a gage volume too large (0.5 mm × 0.5 mm × 20 mm) to capture the detail of the strain gradient. That is reflected in the stresses as well (Fig. 7). The measurement with the large gage volume underestimates the peak stresses by almost 300 MPa!

It should be noted that the gage volumes were nearly the same ((1): 7.2 mm^3, (2): 5 mm^3) but the neutron paths differed. Thus, counting times varied for (1) from 20 min at minimum attenuation to 90 min at maximum attenuation. For (2), the spread was 40 min and 80 min for minimum and maximum attenuation.
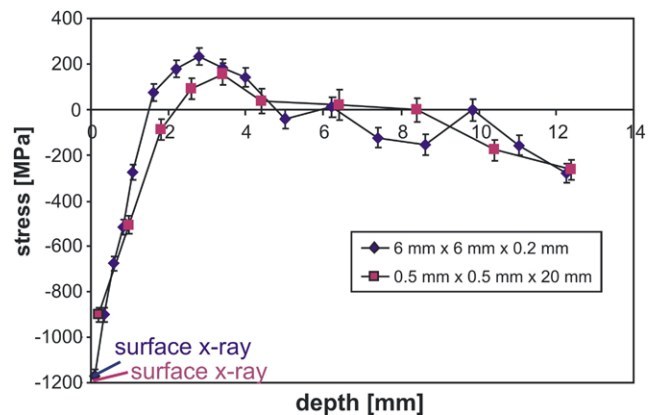

Fig. 7 In-plane stresses for the laser peened sample

4 Conclusions

It was demonstrated that, through adaptation of the shape of the primary beam, through measurement in directions of raised intensity (if preferred orientation exists), and through maintaining the orientation of the gage volume within the sample for all specimen orientations the effective spatial resolution of neutron diffraction strain measurements can be improved down to the order of 0.1 mm. This can be done at data acquisition times <1 h even for medium power (20 MW) neutron sources. The method is particularly well suited for stresses that are homogenous in a plane (sheet metal), and in cases where not large distances to edges and surfaces are required. The demonstrated gain in spatial resolution is to some extent paid for with the need for additional

(and time consuming) reference d-spacing measurements. It is also often necessary to re-measure the surface position after each change in specimen orientation.

References

1. Gnäupel-Herold, T., Haeffner, D.R., Prask, H.J., Matejicek, J.: In: Proceedings of the 6th International Conference on Residual Stresses (ICRS-6), Oxford, July 10–12, 2000, pp. 751–758
2. Gnaeupel-Herold, T., Prask, H.J., Fields, R.J., Foecke, T.J., Xia, Z.C., Lienert, U.: Mater. Sci. Eng. A **366**, 104–113 (2004)
3. Pyzalla, A.: J. Nondestruct. Eval. **19**, 21–31 (2000)
4. Reimers, W., Broda, M., Brusch, G., Dantz, D., Liss, K.-D., Pyzalla, A., Schmackers, T., Tschentscher, T.: J. Nondestruct. Eval. **17**, 129–140 (1998)
5. Luzin, V., Gnäupel-Herold, T., Prask, H.J.: Mater. Sci. Forum **408–412**, 407–412 (2002)
6. Gnaeupel-Herold, T., Foecke, T.J., Prask, H.J., Fields, R.J.: Mater. Sci. Eng. A **399**, 26–32 (2005)
7. Mildner, D.F.R., Chen-Mayer, H.H., Gibson, W.M., Gnäupel-Herold, T., Miller, M.E., Prask, H.J., Schultz, A.J., Vitt, R., Youngman, R.: Rev. Sci. Instrum. **73**, 1985–1993 (2002)
8. Gibson, W.M., Schultz, A.J., Chen-Mayer, H.H., Mildner, D.F.R., Gnäupel-Herold, T., Miller, M.E., Prask, H.J., Vitt, R., Youngman, R., Carpenter, J.M.: J. Appl. Cryst. **35**, 677–683 (2002)
9. Gnäupel-Herold, T.: J. Appl. Cryst. **42**, 192–197 (2009)
10. Wang, X.-L., Spooner, S., Hubbard, C.: J. Appl. Cryst. **30**, 52–59 (1998)
11. Oliveira, M.C., Baptista, A.J., Alves, J.L., Menezes, L.F., Green, D.E., Gnaeupel-Herold, T., Iadicola, M.A., Foecke, T., Stoughton, T.B.: In: Santos, A.D., Barata da Rocha, A. (eds.) Proceedings of the International Deep Drawing Research Group 2006 Conference, June 19–21, 2006, Porto, Portugal, pp. 279–286
12. Green, D.E., Stoughton, T.B., Gnaeupel-Herold, T., Iadicola, M.A., Foecke, T.: In: Santos, A.D., Barata da Rocha, A. (eds.) Proceedings of the International Deep Drawing Research Group 2006 Conference, June 19–21, 2006, Porto, Portugal, pp. 559–566 (2006)
13. Hauk, V. (ed.): Structural and Residual Stress Analysis by Nondestructive Methods. Elsevier, Amsterdam (1997), pp. 178–180
14. Ortner, B., Antretter, T., Hofmann, M., Werner, E.: Mater. Sci. Forum **571–572**, 225–229 (2008)